

doi:10.1016/j.gloplacha.2007.04.002

 ? [Cite or Link Using DOI](#)

Copyright © 2007 Elsevier B.V. All rights reserved.

Land water storage contribution to sea level from GRACE geoid data over 2003–2006

 G. Ramillien^a  , S. Bouhours^a, A. Lombard^a, A. Cazenave^a, F. Flechtner^b and R. Schmidt^b
^aLEGOS, Toulouse, France

^bGFZ, Potsdam, Germany

Received 5 February 2007; revised 16 April 2007; accepted 20 April 2007. Available online 5 May 2007.

Abstract












Seasonal and inter-annual change in land water storage (expressed in terms of water volume change) over 27 large river basins worldwide are estimated from monthly GRACE geoids solutions computed at GFZ from February 2003 to February 2006. The largest annual water volume change is found in the Amazon basin, followed by the Parana, Ob, Orinoco, Tocantins, Niger, Congo, Ganges, Mekong, and Brahmaputra. In terms of trend over the 3-year period, positive and negative values are observed but in a number of cases computed trends are at the noise level. However significant negative trends are found in the Amazon, Ganges, Mississippi, Nile, Parana, and Zambezi basins, indicating water mass loss over that period. Positive trends (water mass gain) are marginally significant. We have computed the land water contribution to sea level change. On average over the 3-year time span, we find that the net effect is positive (net loss of water in terrestrial reservoirs), on the order of 0.19 +/- 0.06 mm/yr. If sustained over a longer time span than considered here, such a value may become comparable to the ice sheets contribution to sea level rise.

Keywords: GRACE; continental water storage; sea level rise; water mass balance

Article Outline

1. [Introduction](#)
2. [GRACE data analysis](#)
 - 2.1. [Data](#)
 - 2.2. [Generalized least-square inversion](#)
3. [Results](#)
4. [Leakage and truncation errors](#)
5. [Discussion](#)
6. [Conclusion](#)

Article Toolbox


-  Download PDF
-  E-mail Article
-  Cited By
-  Save as Citation Alert
-  Citation Feed
-  Export Citation
-  Add to my Quick Links
-  Add to 
-  Permissions & Reprints
-  Cited By in Scopus (2)


Related Articles in ScienceDirect

- [Time variations of land water storage from an inversion...
Earth and Planetary Science Letters](#)
- [Estimation of steric sea level variations from combined...
Earth and Planetary Science Letters](#)
- [Present-day sea level rise: A synthesis
Comptes Rendus Geosciences](#)
- [Contributions of hydrological processes to sea level ch...
Physics and Chemistry of the Earth, Parts A/B/C](#)
- [Annual cycle in mean sea level from Topex-Poseidon and ...
Global and Planetary Change](#)

 ▶ [View More Related Articles](#)
[View Record in Scopus](#)

The research collaboration tool

-   No user rating
-  No user tags yet
-  This article has not yet been bookmarked
-  No comments on this article yet
-  Not yet shared with any groups

 Be the first to add this article in 

References

1. Introduction

In the recent years, much progress has been made in estimating the two main causes of global mean sea level change, e.g., thermal expansion and land ice melt. Change in terrestrial water storage of climate-driven and anthropogenic origin is a third potentially important component to present-day sea level change. However, up to recently, no global terrestrial storage observations were available to quantify this contribution. Global land surface models have allowed computing the climate-driven component of the terrestrial water storage over the past few decades ([Milly et al., 2003] and [Ngo-Duc et al., 2005]). These studies show that time-varying storage of terrestrial waters significantly contribute to sea level at inter-annual and decadal time scales, while no long-term trend is indicated from these modeling approaches. The anthropogenic component is highly uncertain because of the lack of global information on ground water mining, irrigation and artificial reservoirs filling ([Chao, 1995], [Gornitz, 2001] and [Sahagian, 2000]). On the basis of available information, the opposite effects on sea level of reservoir filling and ground water mining almost cancel each other ([Milly et al., 2006]). However, the apparently negligible contribution of human activities remains very poorly known at present.

Since 2002, we have at our disposal a new type of observations for quantifying spatio-temporal change in land water storage: global gravity data from the GRACE space mission. Several studies have demonstrated the capability of GRACE to precisely measure the vertically integrated change in terrestrial water mass over time scales ranging from months to years (e.g. [Tapley et al., 2004a], [Tapley et al., 2004b], [Wahr et al., 2004], [Ramillien et al., 2005] and [Schmidt et al., 2006]). These studies have so far mostly focussed on the seasonal land water signal. In the present paper, we analyse GRACE data to also investigate the inter-annual fluctuations in land water storage in the 27 largest river basins worldwide and estimate their corresponding contribution to sea level.

2. GRACE data analysis

2.1. Data

We have analysed new GRACE geoids (GFZ GRACE Level-2 products, version RL03) recently computed by the GeoForschungsZentrum (GFZ) in Germany ([Flechtner, 2006]). The data analysed in this study consists of 35 sets of spherical harmonics up to degree and order 120, given at monthly interval from February 2003 to February 2006 (June 2003 is missing). Unlike the previous GFZ solutions, these new solutions include more reliable degree 2, order 0 harmonic. As the geoid solutions are provided in a terrestrial reference frame which origin is the earth's center of mass, the degree 1 coefficients are set to zero. In the GRACE data processing performed at GFZ, gravitational attractions of the atmosphere and oceans were taken into account using appropriate data and models (see [Flechtner, 2006]). Depending on the application, the atmospheric and/or the oceanic models (also provided as sets of spherical harmonics) are usually added back to the geoid solutions. In particular, according to [Flechtner (2006)], the atmospheric model removed in the data processing at GFZ should be added back, otherwise artificial trends may contaminate the land water solutions when interpreting directly the geoid data in terms of equivalent water heights (as usually done). However, here we do not directly express the geoid solution in terms of land water storage. Rather, we apply a generalized least squares inversion to separate the geoid signals associated with the different reservoirs (atmosphere, oceans, land); see Section 2.2. Hence, any artificial trend due to atmospheric effects processing by GFZ will not affect the land water solutions based on the inversion, at least at first order (while it may affect the inverse solution of the atmospheric reservoir). Thus we do not add back the atmospheric (nor oceanic) model. We also ignore the degree 1 terms. These terms contribute to signal of wavelength much longer than those considered here (i.e., river basin size).

2.2. Generalized least-square inversion

The numerical strategy for separating the contributions of the different reservoirs was previously presented in (Ramillien et al., 2004) and (Ramillien et al., 2005). It is based on the matrix formalism of the generalized least-squares criteria developed by Tarantola (1987) and consists of estimating separately the spherical harmonic coefficients, in terms of equivalent-water heights, of four different fluid reservoirs (atmosphere, oceans, soil waters and snow pack) from the monthly GRACE geoids. For each water mass reservoir (terrestrial water reservoirs, residual atmosphere and residual ocean), the solution is a linear combination of the coefficients measured by GRACE, of the a priori information from atmospheric/hydrological/oceanic models and optimal coefficients fitting:

$$\Gamma_k(t) = \Gamma_k^0(t) + C_k \Omega (C_D + C_M + \Omega C_k \Omega^T)^{-1} \times [\Gamma^{\text{OBS}}(t) - \Omega \Gamma_k^0(t)] \quad (1)$$

where $\Gamma_k(t)$ is the vector formed by the list of all spherical harmonic coefficients of the geoid to be solved for the k -th contribution and time t , $\Gamma^{\text{OBS}}(t)$ is the vector formed with the geoid coefficients from GRACE, $\Gamma_k^0(t)$ corresponds to the initial solution coefficients vector (i.e. "first guess"). C_D and C_M are the a priori covariance matrices of the GRACE geoid coefficients, and of land surface models, respectively. The latter matrix and the vector $\Gamma_k^0(t)$ are estimated from the geoid coefficients derived from global model outputs for each month. An iteration process was implemented. Convergence is generally obtained after 2 or 3 iterations, but in some cases up to 5 iterations are required. In this study, we assume that the time-varying geoid solutions provided by GFZ at monthly interval over the 3-year time span considered in this study (corrected using atmosphere and oceanic models) correspond mainly to surface mass redistributions (i.e., not to deep solid Earth phenomena). Therefore, the coefficients $\Gamma(t) = (\delta U_{nm}(t), \delta V_{nm}(t))$ of the solution are converted into units of surface mass density (expressed in mm of equivalent-water height) by using an isotropic filter to obtain the spherical harmonics $(\delta C_{nm}(t), \delta S_{nm}(t))$ of the water height solutions (e.g., Wahr et al., 1998; [Ramillien et al., 2004] and [Chao, 2005]):

$$\begin{pmatrix} \delta C_{nm}(t) \\ \delta S_{nm}(t) \end{pmatrix} = \left[\frac{4\pi G \rho_w R}{(2n+1)\bar{\gamma}} (1+k'_n) \right]^{-1} \begin{pmatrix} \delta U_{nm}(t) \\ \delta V_{nm}(t) \end{pmatrix} \quad (2)$$

where n and m are harmonic degree and order respectively. G is the gravitational constant, $\bar{\gamma}$ is the mean gravity acceleration, k'_n is the elastic Love number of degree n , R is the mean Earth's radius (~ 6371 km) and ρ_w is the mean water density (~ 1000 kg/m³).

Water height anomalies $\delta h(\theta, \lambda, t)$ are further computed from the $\Gamma_{nm}(t) = \{\delta C_{nm}(t), \delta S_{nm}(t)\}$ coefficients by computing the linear expansion up to degree N :

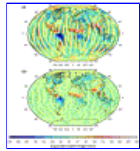
$$\delta h(\theta, \lambda, t) = \sum_{n=1}^N \sum_{m=0}^n \{ \delta C_{nm}(t) \cos(m\lambda) + \delta S_{nm}(t) \sin(m\lambda) \} \tilde{P}_{nm}(\cos\theta) \quad (3)$$

where θ and λ are co-latitude and longitude, respectively. N is the maximum degree of the development. \tilde{P}_{nm} is the associated Legendre function.

To compute the covariance matrix C_M , we use two global land surface models: the Water Gap Hydrological Model (WGHM) (Döll et al., 2003) and the Land Dynamics model (LaD) from Milly and Shmakin (2002). The covariance terms associated with the residual atmospheric and oceanic signals are computed using the difference between two atmospheric and two oceanic models. These model outputs are used for estimating statistical properties of the hydrological parameters (see Ramillien et al., 2005, for details).

In the following, we consider the sum of the soil water and snow solutions (further called land water solutions). The geoid solutions and land water solutions are truncated at $N = 50$ (equivalent wavelength of 400 km). This choice is a compromise between enough spatial resolution (considering the size of the river basins analysed here) and minimization of the high-frequency noise of the geoid solutions.

To illustrate the advantage of the inversion process versus the direct use of the geoid solutions interpreted in terms of land water storage (as done by most investigators), Fig. 1 compares, for October 2003, the geoid solution expressed in equivalent-water height with the inversion solution for the same month. We clearly see that inversion allows to significantly reduce the noise, including the north–south stripes related to tesseral coefficients resonance. The land water signal related to river basins is enhanced after inversion.



Full-size image (128K)

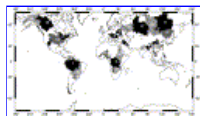
Fig. 1. (a) geoid solution expressed in mm equivalent water height (raw data) for October 2003. (b) same solution after the inversion process.

3. Results

We estimate the change in total water volume (soil and underground water plus snow where appropriate) in 27 river basins (whose location is shown in Fig. 2) from the inversion process described above. The river basin contours are based on masks of 0.5° resolution from Oki and Sud (1998). Only basins of area larger than $400 \times 400 \text{ km}^2$ are considered here, to be homogeneous with the resolution (400 km) of the land water solutions. To estimate the contribution of individual basins, we convolve the land water solution (after inversion and iterations) with the spherical harmonics expansion of the geographical mask used to mark the boundary of the studied area (set to 1 inside the considered region and zero outside). Corresponding water volume variation for each basin is thus given by the scalar product relation:

$$\delta\psi(t) = 4\pi R^2 \sum_{n=1}^N \sum_{m=0}^n \{A_{nm}\delta C_{nm}(t) + B_{nm}\delta S_{nm}(t)\} \quad (4)$$

where A_{nm} and B_{nm} are normalized harmonic coefficients of the river basin mask (discussion of errors associated with the truncation of the basin mask spherical harmonic development is presented in Section 4).

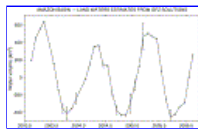


Full-size image (62K)

Fig. 2. River basins considered in this study (numbers as given in Table 1).

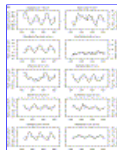
In Fig. 3 the raw water volume time series of the Amazon basin for the 3-year period (Feb. 2003 to Feb. 2006) is presented. Error bars computed a posteriori by the inversion process are also shown. The water volume time series is dominated by a strong seasonal (annual) cycle, of $\sim 400 \text{ km}^3$ amplitude. Some year to year variability is also seen. In Fig. 4 the whole set of water volume time series (27 basins) (arranged in alphabetic order) is presented. In this figure, error bars are not shown for clarity. On the plots are also presented the residual time series, after removing the annual cycle. The largest seasonal water volume variation is found in the Amazon basin (as expected, considering the very large area of this basin), followed by the Parana, Ob, Orinoco, Tocantins, Niger, Congo,

Ganges, Mekong, and Brahmaputra river basins. The residual time series indicate that in some basins, trends may be either negative or positive (although we approximate the residual time series by a linear trend, we are aware that it likely does not reflect a long-term trend, but only inter-annual variability). Water volume trend values and associated uncertainties are gathered in Table 1. The results presented in Table 1 indicate that in many instances, trends are of the same order of magnitude as uncertainties, thus are not significant. However some basins show significant decreasing trends (i.e., water loss) over the 3-year time span: Amazon, Ganges, Mississippi, Nile, Parana, and Zambezi. In the Mississippi basin, the (residual) water volume is stable during 2003–2004, then presents a negative slope as of 2005. Most positive slopes (i.e., water mass gain) are not significant, except for the Siberian basins, Lena and Yenisey. Fig. 5 presents the global trend map computed over the 3-year period (expressed in equivalent water height). We note that in addition to the river basins mentioned above, some regions have also been losing water during the 3-year time span, in particular the East African lakes region. On the other hand, the negative trend seen in the Alaska region is likely related to the ice mass loss of Alaskan glaciers, as shown by Tamisiea et al. (in press) and Chen et al. (2006), while the positive trend observed around the Hudson Bay may reflect glacial isostatic adjustment (GIA) rather than water mass change.



Full-size image (25K)

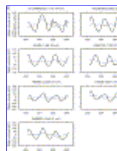
Fig. 3. Amazon water volume time series (and associated error bars) after inversion (units: cu km).



Full-size image (122K)



Full-size image (125K)

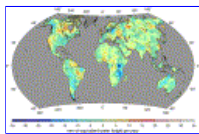


Full-size image (93K)

Fig. 4. Water volume time series (solid line) and residuals (after removing the annual cycle) over the 27 river basins (units: cu km).

Table 1.

N°	River basin	Time interval : Feb. 2003–Feb. 2006		
		Area 10 ⁶ km ²	Water volume trend (km ³ /yr)	Equivalent sea level trend (mm/yr)
1	Amazon	6.21	- 18. +/- 10.	0.05 +/- 0.03
2	Amur	1.88	- 3. +/- 3.5	0.008 +/- 0.009
3	Brahmaputra	0.66	1.8 +/- 1.4	- 0.005 +/- 0.004
4	Colorado	0.64	2.15 +/- 0.7	- 0.006 +/- 0.002
5	Congo	3.82	- 7.2 +/- 10.	0.02 +/- 0.03
6	Danube	0.81	1.5 +/- 1.5	- 0.004 +/- 0.004
7	Dniepr	0.52	1.3 +/- 0.7	- 0.0035 +/- 0.0019
8	Euphrate	0.81	- 3. +/- 1.4	0.008 +/- 0.004
9	Ganges	0.97	- 4.7 +/- 1.8	0.013 +/- 0.005
10	Hwangho	0.73	- 1.8 +/- 0.7	0.005 +/- 0.002
11	Lena	2.74	4.7 +/- 1.8	- 0.013 +/- 0.005
12	Mckenzie	1.73	2.15 +/- 1.8	- 0.006 +/- 0.005
13	Mekong	0.77	- 1.1 +/- 1.8	0.003 +/- 0.005
14	Mississippi	3.3	- 11. +/- 2.9	0.03 +/- 0.01
15	Niger	2.27	7.2 +/- 2.9	- 0.02 +/- 0.01
16	Nile	3.17	- 12.6 +/- 3.5	0.035 +/- 0.009
17	Ob	2.85	1.5 +/- 3.5	- 0.004 +/- 0.009
18	Okavango	0.83	0.55 +/- 0.7	- 0.0015 +/- 0.002
29	Orinoco	0.87	1.8 +/- 0.4	- 0.005 +/- 0.001
20	Parana	2.98	- 14.4 +/- 7.2	0.04 +/- 0.02
21	St-Lawrence	1.12	- 4.3 +/- 3.5	0.012 +/- 0.009
22	Tocantins	0.86	1.5 +/- 2.5	- 0.004 +/- 0.007
23	Volga	1.42	- 0.55 +/- 1.5	0.0015 +/- 0.004
24	Yangtze	1.78	0.35 +/- 1.8	- 0.001 +/- 0.005
25	Yenisey	2.57	3.25 +/- 2.1	- 0.009 +/- 0.006
26	Yukon	0.82	- 3.6 +/- 1.	0.010 +/- 0.003
27	Zambezi	1.39	- 13. +/- 1.8	0.036 +/- 0.005
	Sum		68.5 +/- 21.	0.19 +/- 0.06



[Full-size image \(71K\)](#)

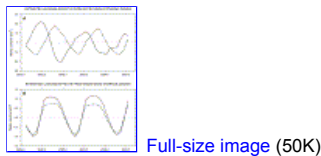
Fig. 5. Trend map computed over the 3-year period (and after inversion), expressed in equivalent water height (units: mm/yr).

We next examine the contribution of land water storage change to sea level (for each river basin, the water volume change is simply divided by the total ocean surface - 360 10⁶ km² —, and opposite sign is assigned). The corresponding sea level trends and associated uncertainties are also gathered in [Table 1](#). We note positive sea level contributions from Amazon, Ganges, Mississippi, Nile, Parana and Zambezi (as mentioned above, these basins have lost water during the 3-year period). On the other hand, the Siberian river basins (Lena and Yenisey) have a slight negative contribution to sea level over this time

span. A similar behaviour is observed for the McKenzie basin in Northwestern Canada. The slight positive contribution of the Yukon basin in Alaska may partly include Alaskan glaciers melting as reported by other studies ([Chen et al., 2006] and [Tamsiea et al., in press]) and other observations (Arendt et al., 2002). The net budget of the 27 basin contributions amounts to $\sim 0.19 \pm 0.06$ mm/yr sea level rise over the 3-year period.

4. Leakage and truncation errors

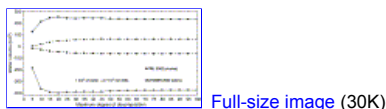
The results presented in Section 3 may be contaminated by two potential source of errors : (1) the contamination effect (or leakage) of gravity signals due to river basins away from the considered basin and (2) the abrupt truncation of the spherical harmonic expansion of the mask. Considering error (1), water mass signals outside the domain limited by the mask may leak into the considered region, and thus pollute the estimated water volume. To estimate, over a given basin, the land hydrology leakage from outside regions, we use monthly global water storage fields based on WGHM (Döll et al., 2003) over the period 2002–2004, and compute the contaminating signal over each basin. The procedure is as follows: (a) synthesis of global $1^\circ \times 1^\circ$ grids of water heights from the monthly coefficients of the WGHM model up to degree 50; (b) set zero values to mask the influence of grid points inside the considered basin; (c) spherical harmonic analysis of these gapped grids to get the corresponding global spherical coefficients; (d) computation of the water volume variations using Eq. (4). We estimate separately the leakage of ground/soil water and snow. The ground water leakage effects in a given basin from other continental water areas are predominantly seasonal. Amplitudes can reach 10% of the estimated water volume signal in the case of Amazon basin. Besides, the impact of the snow leakage is small in general. Fig. 6 shows these effects for two basins: the Amazon and the Mekong. The seasonal ground/soil water leakage is on the order of 5% for the Amazon basin and reaches 15% for the Mekong basin. The smaller the basin area, the larger the leakage effect. As expected, the snow leakage is very small for these two basins located in tropical/equatorial regions. In terms of trend, the leakage is negligible. But we cannot exclude that global land surface models like WGHM are less accurate on inter-annual time scales.



Full-size image (50K)

Fig. 6. (A) Leakage error expressed in water volume due to soil/underground waters over the amazon (solid line) and Mekong basin (dashed line). (B) same as (a) for the snow leakage.

As far as error (2) is concerned, the model data and mask were developed in spherical harmonics, for two months (April 2002 and October 2002) and two basins (Amazon and Mekong), with truncation ranging from degree 5 to 100. Fig. 7 shows the water volume estimate for these two months and two basins, as a function of cut-off degree. We clearly see that truncation at low degree leads to large underestimate of the water volume. However at degree 50, the amplitude is almost stabilized. Compared to a cut-off at degree 100, a degree 50 cut-off only marginally contributes to the error budget. Note that for smaller basins than Amazon and Mekong, the level of error may be slightly larger.



Full-size image (30K)

Fig. 7. Estimate of the water volume (in cu km) for two months (April 2002: black circles; October 2002: stars) and two basins (Amazon: solid line; Mekong: dashed line) as a function of cut-off degree.

5. Discussion

Satellite altimetry observations since 1993 indicate that sea level has been rising by $\sim 3.3 \pm 0.4$ mm/yr (update from [Cazenave and Nerem, 2004] and [Nerem et al., 2006]). Knowledge of the contributions of thermal expansion, glaciers melting and mass change of the ice sheets has considerably improved in the recent years. Contribution of thermal expansion amounts to 1.5 ± 0.3 mm/yr for the last decade ([Willis et al., 2004], [Levitus et al., 2005], [Ishii et al., 2006] and [Lombard et al., 2006]) while the contribution of glaciers is estimated to 0.8 ± 0.3 mm/yr ([Dyurgerov and Meier, 2005]). Remote sensing and other observations have recently resulted in direct estimates of the mass balance of Greenland and Antarctica ([Rignot and Thomas, 2002], [Thomas et al., 2004], [Johannessen et al., 2005], [Zwally et al., 2005], [Davis et al., 2005], [Velicogna and Wahr, 2005], [Velicogna and Wahr, 2006], [Rignot and Kanagaratnam, 2006], [Chen et al., 2006], [Ramillien et al., 2006] and [Luthcke et al., 2006]; see also Cazenave, 2006 for a summary). Although considerable uncertainty exists for both ice sheets due to incomplete coverage in space and time by the combined observing strategies, a rough estimate of the Greenland ice sheet contribution to sea level rise is $\sim 0.3 \pm 0.15$ mm/yr for the recent years, while the Antarctica ice sheet may be close to balance (a small contribution of ~ 0.1 mm/yr is assumed). Summing up these various contributions leads to $\sim 2.7 \pm 0.4$ mm/yr for the climate-related factors. This leaves about 0.6 mm/yr unexplained. This residual includes the terrestrial water storage contribution.

Although the 3-year terrestrial water trend estimated in the present study from GRACE may not directly compare to the above residual trend over the past decade or so, we note that its order of magnitude (~ 0.2 mm/yr) can explain part of the missing signal. The 0.19 ± 0.06 mm/yr trend estimate from GRACE over the past 3 years is also of similar magnitude than land surface model estimates. Milly et al. (2003) used the Land Dynamics model to quantify the contributions of time-varying storage of terrestrial waters to sea level rise in response to climate change on inter-annual to decadal time scales. A small positive sea level trend of 0.12 mm/yr was estimated for the period 1981–2000, and 0.18 mm/yr for the 1990s. The long-term trend was very small, and large inter-annual/decadal fluctuations dominated the signal. Subsurface water was the major contributor on inter-annual time scales. The study of Ngo-Duc et al. (2005) based on the ORCHIDEE land surface model over 1950–2000 also found negligible long-term contribution but large inter-annual fluctuations, of the same order of magnitude as found in this study (decadal fluctuations being larger. Ngo-Duc et al. (2005) showed that inter-annual variability in land water storage was mainly caused by change in precipitation in tropical river basins, with periods of increased rainfall corresponding to increased water mass stored in terrestrial reservoirs, thus to sea level fall, and inversely. Further investigation is clearly needed to establish whether the change in water mass in large river basins reported in the present study from GRACE observations is indeed related to precipitation change, or if other factors (e.g., change in runoff) are also important.

6. Conclusion

Up to recently, the land water contribution to sea level rise due to climate variability could not be estimated because of lack of global in situ observations. The anthropogenic component of land water storage (due to dam building, irrigation, ground water mining) is also almost totally unknown (e.g., Milly et al., 2006). GRACE is now able to measure the sum of these two contributions. In the present study, we find that the GRACE-based sea level trend due to land water storage may partly contribute to closing the sea level budget over the recent years. Of course, the time span (3 years) considered here is very short, so that we cannot conclude that the 0.2 mm/yr contribution to sea level rise represents the long-term contribution of terrestrial waters. At best, it represents an inter-annual fluctuation. This is why extending the GRACE time series with improved processing that allows reducing the current noise level is a major goal for the near future.

References

- Arendt et al., 2002** A.A. Arendt, K.A. Echelmeyer, W.D. Harrison, C.S. Lingle and V.B. Valentine, Rapid wastage of Alaska glaciers and their contribution to rising sea level, *Science* **297** (2002), pp. 382–386. [Full Text via CrossRef](#) | [View Record in Scopus](#) | [Cited By in Scopus \(155\)](#)
- Cazenave, 2006** A. Cazenave, How fast are Greenland and Antarctica losing ice mass?, *Science* **314** (2006), pp. 1250–1252. [Full Text via CrossRef](#) | [View Record in Scopus](#) | [Cited By in Scopus \(7\)](#)
- Cazenave and Nerem, 2004** A. Cazenave and R.S. Nerem, Present-day sea level change: observations and causes, *Review of Geophysics* **42** (2004), p. RG3001 doi: 8755-1209/04/2003RG000139. [Full Text via CrossRef](#) | [View Record in Scopus](#) | [Cited By in Scopus \(92\)](#)
- Chao, 1995** B.F. Chao, Anthropogenic impact on global geodynamics due to reservoir water impoundment, *Geophys. Res. Lett.* **22** (1995), pp. 3529–3532. [Full Text via CrossRef](#) | [View Record in Scopus](#) | [Cited By in Scopus \(17\)](#)
- Chao, 2005** B.F. Chao, On inversion for mass distribution from global (time-variable) gravity field, *J. Geodyn.* **39** (2005), pp. 223–230. [Article](#) |  [PDF \(87 K\)](#) | [View Record in Scopus](#) | [Cited By in Scopus \(13\)](#)
- Chen et al., 2006** J.L. Chen, C.R. Wilson and B.D. Tapley, Satellite gravity measurements confirm accelerated melting of the Greenland ice sheet, *Science* **313** (2006), p. 1958. [Full Text via CrossRef](#) | [View Record in Scopus](#) | [Cited By in Scopus \(36\)](#)
- Davis et al., 2005** Davis *et al.*, Snowfall-driven growth in East Antarctica ice sheet mitigates recent sea level rise, *Science* **308** (2005), pp. 1898–1907.
- Döll et al., 2003** P.F. Döll, F. Kaspar and B. Kaspar, A global hydrological model for deriving water availability indicators: model tuning and validation, *J. Hydrol.* **270** (2003), pp. 105–134. [Article](#) |  [PDF \(1483 K\)](#) | [View Record in Scopus](#) | [Cited By in Scopus \(73\)](#)
- Dyrugerov and Meier, 2005** M. Dyrugerov and M.F. Meier, *Glaciers and Changing Earth System: a 2004 snapshot*, INSTAAR, Boulder (2005).
- Flechtner, 2006** F. Flechtner, Grace Science Data System Monthly Report, Tech. Report (2006) Dec..
- Gornitz, 2001** V. Gornitz, Impoundment, groundwater mining, and other hydrologic transformations: impacts on global sea level rise. In: B.C. Douglas, M.S. Kearney and S.P. Leatherman, Editors, *Sea Level Rise, History and Consequences*, Academic Press, San Diego (2001) pp. 97–119.
- Ishii et al., 2006** M. Ishii, M. Kimoto, K. Sakamoto and S.I. Iwasaki, Steric sea level changes estimated from historical ocean subsurface temperature and salinity analyses, *J. Oceanogr.* **62** (2006), pp. 155–170. [Full Text via CrossRef](#) | [View Record in Scopus](#) | [Cited By in Scopus \(36\)](#)
- Johannessen et al., 2005** O.M. Johannessen, K. Khvorostovsky, M.W. Miles and L.P. Bobylev, Recent ice sheet growth in the interior of Greenland, *Science* **310** (2005), pp. 1013–1016. [View Record in Scopus](#) | [Cited By in Scopus \(37\)](#)
- Levitus et al., 2005** S. Levitus, J.I. Antonov and T.P. Boyer, Warming of the World Ocean, 1955–2003, *Geophys. Res. Lett.* **32** (2005), p. L02604. [Full Text via CrossRef](#)
- Lombard et al., 2006** A. Lombard, A. Cazenave, S. Guinehut, P.-Y. Le Traon and C. Cabanes, Perspectives on present-day sea level change, *Ocean Dyn., Ocean Dynamics*

(2006) published online.

[Luthcke et al., 2006](#) S.B. Luthcke, H.J. Zwally, W. Abdalati, D.D. Rowlands, R.D. Ray, R.S. Nerem, F.G. Lemoine, J.J. McCarthy and D.S. Chinn, Recent Greenland ice mass loss by drainage system from satellite gravimetry observations, *Scienceexpress* (2006) 10.1126/science.1130776.

[Milly and Shmakin, 2002](#) P.C.D. Milly and A.B. Shmakin, Global modeling of land water and energy balances. Part I: the Land Dynamics (LaD) model, *J. Hydrometeorol.* **3** (2002), pp. 283–299. [Full Text via CrossRef](#) | [View Record in Scopus](#) | [Cited By in Scopus \(99\)](#)

[Milly et al., 2003](#) P.C.D. Milly, A. Cazenave and M.C. Gennero, Contribution of climate-driven change in continental water storage to recent sea-level rise, *Proc. Natl. Acad. Sci.* **100** (2003), pp. 13158–13161. [Full Text via CrossRef](#) | [View Record in Scopus](#) | [Cited By in Scopus \(21\)](#)


[Milly et al., 2006](#) P.C.D. Milly, A. Cazenave, J. Famiglietti, V. Gornitz, K. Laval, D. Lettenmaier, D. Sahagian, J. Wahr and C. Wilson, Terrestrial water storage contributions to sea level rise and variability, *Proceedings of the WCRP workshop 'Understanding sea level rise and variability*, UNESCO, Paris (2006).


[Nerem et al., 2006](#) S. Nerem, E. Leuliette and A. Cazenave, Present-day sea level change, *C. R. Geosci.* **338** (2006), pp. 1077–1083 issue 14–15.

[Ngo-Duc et al., 2005](#) T. Ngo-Duc, K. Laval, Y. Polcher, A. Lombard and A. Cazenave, Effects of the land water storage on the global mean sea level over the last half century, *Geophys. Res. Lett.* **32** (2005), p. L09704. [Full Text via CrossRef](#)

[Oki and Sud, 1998](#) T. Oki and Y.C. Sud, Design of Total Runoff Integrating Pathways (TRIP) — a global river channel network, *Earth Interact.* **2** (1) (1998), pp. 1–37. [Full Text via CrossRef](#)


[Ramillien et al., 2004](#) G. Ramillien, A. Cazenave and O. Brunau, Global time-variations of hydrological signals from GRACE satellite gravimetry, *Geophys. J. Int.* **158** (2004), pp. 813–826. [Full Text via CrossRef](#) | [View Record in Scopus](#) | [Cited By in Scopus \(18\)](#)

[Ramillien et al., 2005](#) G. Ramillien, F. Frappart, A. Cazenave and A. Güntner, Time variations of the land water storage from an inversion of 2 years of GRACE geoids, *Earth Planet. Sci. Lett.* **235** (2005), pp. 283–301. [Article](#) |  [PDF \(2601 K\)](#) | [View Record in Scopus](#) | [Cited By in Scopus \(30\)](#)

[Ramillien et al., 2006](#) G. Ramillien, A. Lombard, A. Cazenave, E.R. Ivins, M. Llubes, F. Remy and R. Biancale, Interannual variations of the mass balance of the Antarctica and Greenland ice sheets from GRACE, *Glob. Planet. Change* **53** (2006), pp. 198–208. [Article](#) |  [PDF \(770 K\)](#) | [View Record in Scopus](#) | [Cited By in Scopus \(21\)](#)

[Rignot and Kanagaratnam, 2006](#) E. Rignot and P. Kanagaratnam, Changes in the velocity structure of the Greenland ice sheet, *Science* **311** (2006), pp. 986–990. [Full Text via CrossRef](#) | [View Record in Scopus](#) | [Cited By in Scopus \(148\)](#)

[Rignot and Thomas, 2002](#) E. Rignot and R. Thomas, Mass balance of polar ice sheets, *Science* **297** (2002), pp. 1502–1506. [Full Text via CrossRef](#) | [View Record in Scopus](#) | [Cited By in Scopus \(130\)](#)

[Sahagian, 2000](#) D. Sahagian, Global physical effects of anthropogenic hydrological alterations: sea level and water redistribution, *Global Planet. Change* **25** (2000), pp. 39–48. [Article](#) |  [PDF \(98 K\)](#) | [View Record in Scopus](#) | [Cited By in Scopus \(13\)](#)

[Schmidt et al., 2006](#) R. Schmidt, F. Flechtner, C. Reigber, P. Schwintzer, A. Güntner, P. Doll, G. Ramillien, A. Cazenave, S. Petrovic, H. Jochman and J. Wunsch, GRACE

observations of changes in continental water storage, *Glob. Planet. Change* **50/1–2** (2006), pp. 112–126. [Article](#) |  [PDF \(2540 K\)](#) | [View Record in Scopus](#) | [Cited By in Scopus \(27\)](#)

[Tamisiea et al., in press](#) Tamisiea M.E., Mitrovica J.X., Nerem R.S., Leuliette E.W., Milne G.A., in press. Correcting satellite-derived estimates of global mean sea level change for glacial isostatic adjustment, *Geophys. J. Int.*

[Tapley et al., 2004a](#) B.D. Tapley, S. Bettadpur, M. Watkins and C. Reigber, The gravity recovery and climate experiment: mission overview and early results, *Geophys. Res. Lett.* **31** (2004), p. L09607. [Full Text via CrossRef](#) | [View Record in Scopus](#) | [Cited By in Scopus \(190\)](#)

[Tapley et al., 2004b](#) B.D. Tapley, S. Bettadpur, J.C. Ries, P.F. Thompson and M. Watkins, GRACE measurements of mass variability in the Earth system, *Science* **305** (2004), pp. 503–505. [Full Text via CrossRef](#) | [View Record in Scopus](#) | [Cited By in Scopus \(162\)](#)

[Tarantola, 1987](#) A. Tarantola, *Inverse Problem Theory*, Elsevier, Amsterdam (1987) 613 pp..

[Thomas et al., 2004](#) R. Thomas, E. Rignot, G. Casassa, P. Kanagaratnam, C. Acuna, T. Akins, H. Brecher, E. Frederick, P. Gogineni, W. Krabill, S. Manizade, H. Ramamoorthy, A. Rivera, R. Russell, J. Sonntag, R. Swift, J. Yungel and J. Zwally, Accelerated sea level rise from West Antarctica, *Science* **306** (2004), pp. 255–258. [Full Text via CrossRef](#) | [View Record in Scopus](#) | [Cited By in Scopus \(95\)](#)

[Velicogna and Wahr, 2005](#) I. Velicogna and J. Wahr, Greenland mass balance from GRACE, *Geophys. Res. Lett.* **32** (2005), p. L18505. [Full Text via CrossRef](#) | [View Record in Scopus](#) | [Cited By in Scopus \(29\)](#)

[Velicogna and Wahr, 2006](#) I. Velicogna and J. Wahr, Measurements of time-variable gravity show mass loss in Antarctica, *Scienceexpress* (2006) 2 March.

[Wahr et al., 1998](#) J. Wahr, M. Molenaar and F. Bryan, Time variability of the Earth's gravity field: hydrological and oceanic effects and their possible detection using GRACE, *J. Geophys. Res.* **103** (1998), pp. 30205–30229. [Full Text via CrossRef](#) | [View Record in Scopus](#) | [Cited By in Scopus \(229\)](#)

[Wahr et al., 2004](#) J. Wahr, S. Swenson, V. Zlotnicki and I. Velicogna, Time-variable gravity from GRACE: first results, *Geophys. Res. Lett.* **31** (2004), p. L11501. [Full Text via CrossRef](#) | [View Record in Scopus](#) | [Cited By in Scopus \(128\)](#)

[Willis et al., 2004](#) J.K. Willis, D. Roemmich and B. Cornuelle, Interannual variability in upper-ocean heat content, temperature and thermosteric expansion on global scales, *J. Geophys. Res.* **109** (C12036) (2004).

[Zwally et al., 2005](#) H.J. Zwally, M.B. Giovinetto, J. Li, H.G. Cornejo, M.A. Beckley, A.C. Brenner, J.L. Saba and D. Yi, Mass changes of the Greenland and Antarctica ice sheets and shelves and contributions to sea level rise: 1992–2002, *J. Glaciol.* **51** (2005), pp. 509–524.



Corresponding author. LEGOS UMR5566 - Observatoire Midi-Pyrénées, 14-18, Avenue Edouard Belin, F-31401 Toulouse, Cedex 01, France.

Global and Planetary Change
Volume 60, Issues 3-4, February 2008, Pages 381-392

[Home](#) [Browse](#) [Search](#) [My Settings](#) [Alerts](#) [Help](#)



[About ScienceDirect](#) | [Contact Us](#) | [Information for Advertisers](#) | [Terms & Conditions](#) | [Privacy Policy](#)

Copyright © 2008 Elsevier B.V. All rights reserved. ScienceDirect® is a registered trademark of Elsevier B.V.